Chinese Journal of
POLYMER SCIENCE

ARTICLE

https://doi.org/10.1007/s10118-020-2377-y
Chinese J. Polym. Sci. **2020**, *38*, 759–768

Highly Soluble Polyimides Containing Di-*tert*-butylbenzene and Dimethyl Groups with Good Gas Separation Properties and Optical Transparency

Chen-Yi Wang[a*], Cai-Rong Jiang[a], Bin Yu[a], Xiao-Yan Zhao[a*], Zhao-Liang Cui[b], Jian Li[a], and Qiang Ren[a]

[a] *Jiangsu Collaborative Innovation Center of Photovoltaic Science and Engineering, Jiangsu Key Laboratory of Environmentally Friendly Polymeric Materials, School of Materials Science and Engineering, Changzhou University, Changzhou 213164, China*
[b] *State Key Laboratory of Materials-Oriented Chemical Engineering, College of Chemical Engineering, Nanjing Tech University, Nanjing 210009, China*

Abstract A rigid aromatic diamine monomer containing di-*tert*-butylbenzene and dimethyl groups, 3,3′-dimethyl-4,4′-diaminophenyl- 3″,5″-di-*tert*-butyltoluene, was successfully synthesized by a simple coupling reaction using 3,5-di-*tert*-butylbenzaldehyde and *o*-toluidine as starting materials. A series of novel polyimides (**PI 3a**–**3c**) with large pendant groups were prepared with the obtained diamine monomer and three different commercial aromatic dianhydrides (3,3′,4,4′-biphenyltetracarboxylic dianhydride, 4,4′-oxydiphthalic anhydride, and 4,4′-(hexafluoroisopropylidene)diphthalic anhydride) by one-step high temperature polycondensation. The prepared polyimides exhibited high solubility and good membrane forming ability: they could be dissolved not only in some high boiling solvents such as DMF, NMP, DMAc, and *m*-Cresol at room temperature, but also in some low boiling solvents such as $CHCl_3$, CH_2Cl_2, and THF. Their solubility in most solvents could exceed 10 wt%, and the flexible membranes could be obtained by casting their solutions. The prepared membranes exhibited good gas separation properties. The permeability coefficients of **PI 3c** for CO_2 and O_2 were up to 124.6 and 42.8 barrer, respectively, and the selectivity coefficients for CO_2/CH_4 and O_2/N_2 were 14.7 and 3.3, respectively. The membranes had light color and good optical transmission. Their optical transmittance at 450 nm wavelength was in the range of 67%–79%, and the cutoff wavelength was in the range of 310–348 nm. They also had good thermal properties with glass transition temperature (T_g) values in the range of 264–302 °C. In addition, these membranes possessed good mechanical properties with tensile strength ranging between 77.8–87.4 MPa, initial modulus ranging between 1.69–1.82 GPa, and elongation at break ranging between 4.8%–6.1%.

Keywords Polyimides; Di-*tert*-butyltoluene; Gas separation performance; Optical transparency

Citation: Wang, C. Y.; Jiang, C. R.; Yu, B.; Zhao, X. Y.; Cui, Z. L.; Li, J.; Ren, Q. Highly soluble polyimides containing di-*tert*-butylbenzene and dimethyl groups with good gas separation properties and optical transparency. *Chinese J. Polym. Sci.* **2020**, *38*, 759–768.

INTRODUCTION

Due to their unique chemical structures, polyimides (PIs) usually have excellent thermal, mechanical, dielectric and electrical properties, which make them exhibit high potential application value in the fields of microelectronics, aerospace, liquid crystal displays, and gas separation membranes.[1–6] In recent decades, with the research of the synthesis methodology of polyimides, their application in various fields has been further promoted effectively. However, due to the rigidity and regularity of their molecular structures, the commercially available polyimides are generally difficult to dissolve and melt, which makes them unconducive to process into membranes. Meanwhile, when the conventional polyimides are used as gas separation membranes, they usually have low permeability coefficient due to the close packing of molecular chains. For example, the permeability coefficients of Kapton for CO_2 and O_2 are only 3.51 and 5.82 barrer, respectively, and the permeability coefficients of Matrimid for CO_2 and O_2 are just 8.70 and 7.04 barrer, respectively.[7] Such low permeability makes it difficult for them to meet the development needs of modern high-efficiency gas separation equipment. In addition, conventional polyimide membrane materials often exhibit deeper color and poor optical transparency due to the high degree of aromatic conjugation and charge-transfer complex in the polymer molecular chain, affecting their applications in the field of some optoelectronics.[8,9]

In order to further improve the membrane-forming ability, gas separation properties, and optical transparency, it is necessary to reasonably design the structure of polyimides, which plays a key role in their performance.[10–12] It has been found that the intermolecular distance can be effectively increased by introducing rigid structure units with large substituted pendant groups into the molecular structure of polyimides. Also, the close packing and interaction between the macromolecular chains would be weakened, which is very

* Corresponding authors, E-mail: wangcy@cczu.edu.cn (C.Y.W.)
E-mail: zhaoxiaoyan@cczu.edu.cn (X.Y.Z.)

Received October 26, 2019; Accepted November 28, 2019; Published online February 18, 2020

helpful to improve the solubility and membrane-forming ability of polyimides.[13–16] Meanwhile, with the introduction of rigid large substituted side groups and the increase of free volume, the gas separation performance of polyimide membranes will be effectively improved.[17–21] Furthermore, the introduction of large substituted rigid structure units can also reduce the aromatic conjugation of the molecular chains and effectively improve the optical transparency of the membrane material.[22] Among some reported polyimide membranes containing large substituted side group structures, the polyimides containing pendant *tert*-butyl structures exhibit a good overall performance. For instance, Sulub *et al.* designed and synthesized an aromatic dianhydrides containing *tert*-butyl structures through a three-step organic reaction.[23] The related polyimides were able to be dissolved in some common organic solvents and the polymer membranes could be obtained by directly casting their solutions. Their permeability coefficient for O_2 and selectivity coefficient for O_2/N_2 reached up to 34 barrer and 3.5, respectively. Zhang *et al.* reported an aromatic dianhydride monomer containing *tert*-butyl structure by nucleophilic substitution reaction.[24] The permeability coefficient for O_2 and the selectivity separation coefficient for O_2/N_2 of the prepared polyimides were 11.3 barrer and 4.6, respectively. From the perspective of structural design, it can be predicted that if more *tert*-butyl or other large side groups could be introduced into the molecular structure of the polymer, the free volume would be further increased, so as to further improve the solubility and gas separation performance of polyimide. However, due to the challenges in structure design and synthesis methodology, monomers and their polyimides with more *tert*-butyl groups are still few reported. Moreover, most of these monomers and their polyimides with *tert*-butyl structures need to be prepared by multi-step organic reactions, which is complicated for practical industrial applications. Therefore, it is of great significance to design and develop novel polyimides with *tert*-butyl structures and further improve the properties of polyimide membranes. Based on this view, this study reported a rigid aromatic diamine and its polyimide membranes containing di-*tert*-butylbenzene and dimethyl groups by a convenient synthesis method. The solubility, membrane formation, thermal stability, mechanical, optical, and gas separation properties of the polyimide membranes were systematically studied. The introduction of large substituted side groups and rigid diamine structures is expected to give the prepared polyimides excellent comprehensive properties. Meanwhile, the properties of the polyimide membranes were compared with those of other polyimide membranes, and the relationship between the structure and properties of different polyimides was further revealed. This study provided a new strategy and method for the design and preparation of high performance polyimide membranes with *tert*-butyl structure.

EXPERIMENTAL

Materials

3,5-Di-*tert*-butylbenzaldehyde (98%) and *o*-toluidine (98%) purchased from TCI were used directly. Available aromatic tetracarboxylic dianhydrides such as 3,3′,4,4′-biphenyltetracarboxylic dianhydride (BPDA or **2a**), 4,4′-oxydiphthalic dianhydride (ODPA or **2b**), and 4,4′-(hexafluoroisopropylidene)diphthalic anhydride (6FDA or **2c**) were all further purified by recrystallization and dried in vacuo at 200 °C for 6 h before use. Commercially available *N*-methyl-2-pyrrolidinone (NMP), *m*-cresol, *N*,*N*-dimethylacetamide (DMAc), *N*,*N*-dimethylformamide (DMF), dimethyl sulfoxide (DMSO), tetrahydrofuran (THF), and other reagents were all purchased from commercial sources and used directly.

Synthesis of 3,3′-Dimethyl-4,4′-diaminophenyl-3″,5″-di-*tert*-butyltoluene (1)

3,5-Di-*tert*-butylbenzaldehyde (19.62 g, 0.26 mol) and *o*-toluidine (27.82 g, 0.09 mol) were added to a 250 mL three-necked flask under nitrogen atmosphere. After the mixture was stirred to homogeneous, 6 mL of concentrated hydrochloric acid was added in three batches by drops, and the temperature was further raised to 160 °C. The reaction was continued under stirring for another 8 h and then cooled to room temperature. Then the mixture was poured and dispersed in an appropriate amount of ethanol, and an appropriate amount of 15% sodium hydroxide solution was added to adjust the pH ≥ 7. The lower layer of water was separated by liquid separation, and further filtered to obtain a solid powdery preliminary product. After the initial product was dried, it was recrystallized twice with toluene to obtain a white crystalline diamine monomer. (Yield: 85.3%; mp: 188–189 °C).

FTIR (KBr, ν, cm^{-1}): 3480, 3456, 3373, 2961, 2862, 1619, 1593, 1503, 1454, 1360, 1250, 1149, 877, 713, and 624. ^{1}H-NMR (400 MHz, DMSO-d_6, δ, ppm): 1.20 (s, 18H), 1.97 (s, 6H), 4.62 (s, 4H), 5.08 (s, H), 6.48 (d, 2H), 6.56 (d, 2H), 6.68 (s, 2H), 6.96 (s, 2H), 7.17 (s, H). ^{13}C-NMR (100 MHz, DMSO-d_6, δ, ppm): 18.16 (Ce), 31.58 (Cm), 34.93 (Cl), 55.91 (Ca), 114.33 (Cg), 119.38 (Ck), 121.04 (Cd), 123.54 (Cn), 127.48 (Ch), 131.10 (Cc), 133.34 (Cb), 144.52 (Cf), 144.93 (Ci), 149.84 (Cj).

Polymer Synthesis

Taking **PI 3c** as an example, the preparation process is as follows. Specifically, 1.6585 g (0.004 mol) of diamine monomer **1**, 1.7770 g (0.004 mol) of 4,4′-(hexafluoroisopropylidene) diphthalic anhydride, and 12 mL of *m*-cresol were added to a 100 mL flask, and the mixture was stirred for about 0.5 h at 100 °C in nitrogen atmosphere. After the mixture formed homogeneous solution, 6–8 drops of isoquinoline was added, and the mixture was heated up to 195 °C, stirred for another 9 h to obtain viscous polymer solution. Then an appropriate amount of solvent was added to dilute the polymer solution. The filamentous polymer was obtained by precipitating the solution in ethanol. The polymer was soaked in ethanol and hot water for several times to remove the residual solvent in the polymer. The final product **PI 3c** was obtained by filtration and drying.

PI 3a: FTIR (KBr, ν, cm^{-1}): 2962, 2866, 1779, 1724, 1608, 1502, 1474, 1373, 1275, 1239, 1103, 851, 815, and 749. ^{1}H-NMR (400 MHz, DMSO-d_6, δ, ppm): 1.32 (s, 18H), 2.18 (s, 6H), 5.82 (s, H), 7.16 (s, 2H), 7.18 (s, H), 7.32 (s, H), 7.38 (d, 2H), 7.41 (d, 2H), 8.21 (d, 2H), 8.46 (d, 2H), 8.52 (s, 2H).

PI 3b: FTIR (KBr, ν, cm^{-1}): 2962, 2867, 1771, 1724, 1623, 1598, 1502, 1373, 1254, 1230, 1105, 843, 743, and 723. ^{1}H-NMR (400 MHz, DMSO-d_6, δ, ppm): 1.46 (s, 18H), 2.14 (s, 6H), 5.48 (s, H), 7.23 (s, 2H), 7.26 (s, H), 7.52 (s, H), 7.58 (d, 2H), 7.61 (d, 2H), 7.89 (s, 2H), 7.92 (d, 2H), 8.13 (d, 2H).

https://doi.org/10.1007/s10118-020-2377-y

PI 3c: FTIR (KBr, ν, cm^{-1}): 2968, 2861, 1769, 1735, 1620, 1592, 1510, 1380, 1250, 1242, 1120, 856, 753, and 718. ^{1}H-NMR (400 MHz, DMSO-d_6, δ, ppm): 1.24 (s, 18H), 2.16 (s, 6H), 5.64 (s, H), 7.02 (s, 2H), 7.09 (s, H), 7.12 (s, H), 7.23 (d, 2H), 7.36 (d, 2H), 7.76 (d, 2H), 7.92 (d, 2H), 8.23 (s, 2H).

Preparation of PI Membranes

A series of flexible polyimide membranes with controllable thickness were prepared by glass plate coating. At first, about 0.6 g of polymer resin was dissolved in 15 mL of DMAc. The solution was filtered with a needle filter and poured into a glass mould. The solvent was evaporated and dried in an oven at 70–80 °C. After 12 h, the obtained membrane was placed in a vacuum oven at 200 °C to continue drying for another 12 h, and the residual solvent was removed to obtain a film with a thickness of about 70 μm, which is used to test mechanical properties, thermal properties, and gas separation performance. The membrane thickness used for optical performance test was about 20 μm.

Measurements

The structures of the prepared diamine monomer and polymers were characterized using a Nicolet Magna Model 370 infrared spectrometer from Nicolet, USA. Among them, the diamine monomer was subjected to tableting test with KBr, and the polymers were tested by membrane. Ultraviolet-visible absorption spectra of polymer membranes were measured by Lambda 950 ultraviolet-visible spectrophotometer of Perkin Elmer Company, USA, where the wavelength ranges from 200 nm to 800 nm. Nuclear magnetic resonance analyses of monomer and polymers were carried out using an ARX-400 NMR spectrometer from Bruker, Switzerland. The monomer and the polymers were treated with DMSO-d_6 as the solvent, and the internal standard was tetramethylsilane (TMS). The molecular weights of polymers were tested by WATERS 1515 gel permeation chromatography (GPC). The monodisperse polystyrene was used as the standard sample and THF as the eluent, the flow rate was 1 mL·min^{-1}, and the oven and detector temperatures were 35 °C. The intrinsic viscosity was measured in a constant temperature flume at 30 °C by dissolving the polymer in NMP and preparing a solution of 0.5 g·dL^{-1}. The thermal decomposition temperature was measured using Perkin-Elmer TGA-7 thermogravimetric differential scanning calorimeter of Perkin Elmer Company, USA. The temperature range was 50–800 °C with the heating rate of 20 °C·min^{-1} in N_2 and air, respectively. Differential scanning calorimetry (DSC) of NETZSCH DSC 200PC was used to analyze 9 ± 1 mg of samples. The glass transition temperature (T_g) was determined at the heating rate of 20 °C·min^{-1} and was taken at the midpoint of the baseline slope change during the second DSC thermal scanning. The solubility of polymers was determined by observing the solubility of 100 mg sample in 1 mL of organic solvent for 24 h. Samples not directly dissolved were then heated. Solubility could be divided into room temperature soluble, heating soluble, and insoluble according to the dissolution. The mechanical properties of a series of polymer membranes were tested under a tensile load of 5 kN and a tensile rate of 5 mm·min^{-1} using AGS-500ND tensile test machine of Shimadzu Corporation of Japan. Wide-angle X-ray diffraction (WAXD) was measured by D/max 2500PC X-ray diffractometer produced by Nippon Science Company. The polymer membrane was spread on a hollow glass plate with a certain thickness. The ray source was copper target and the angle of 2θ was 5°–60°. The Bragg's equation ($d = \gamma/2\sin\theta$) was used for calculation. The permeability of polymer film to different gases (CO_2, O_2, N_2, and CH_4) was measured using a MKS Baratron instrument. The applied gas pressure was 0.35 MPa and the temperature was 35 °C. The permeation device was designed and the detailed experimental steps were carried out in accordance with the literature method.[25] The gas permeability of membranes was tested by constant pressure-variable volume method combined with gas chromatography. The permeability of the gas can be calculated according to the following formula:

$$P = \frac{F}{A\Delta p/L}$$

where F is gas flow (cm^3(STP)·min^{-1}); A is the effective area of the membrane (cm^2); Δp is pressure difference between the upper and lower sides of the membrane (cmHg); L is the thickness of the membrane (cm).

Permeability of each pure gas is obtained from the average of at least three tests. Free volume (FFV) is calculated using the following formula:

$$\mathrm{FFV} = (V - V_0)/V$$
$$V = M/\rho$$
$$V_0 = 1.3V_W$$

where V is the specific volume; M is the molar mass (g·mol^{-1}) of the monomer repeat unit; ρ is the density of the membrane (g·cm^{-1}); V_W is the specific van der Waals volume calculated using the Bondi's group contribution method.[26,27]

RESULTS AND DISCUSSION

Synthesis of Aromatic Diamine Monomer

Scheme 1 shows the synthetic route to diamine monomer containing both di-*tert*-butyl and dimethyl groups. The coupling reaction of 3,5-di-*tert*-butylbenzaldehyde and *o*-toluidine was carried out in reflux under concentrated hydrochloric acid catalysis. The novel rigid aromatic diamine monomer, 3,3′-dimethyl-4,4′-diaminophenyl-3″,5″-di-*tert*-butyltoluene (**1**), was obtained by the dispersion and precipitation in ethanol and further recrystallized in toluene. Hydrochloric acid can not only be used as a catalyst, but also form ammonium salts with *o*-toluidine, which further increases the solubility of the product.

The chemical structure of diamine monomer was characterized by FTIR, ^{1}H- and ^{13}C-NMR spectra. Fig. 1 is the FTIR spectrum of diamine **1**. It can be seen from the spectrum that there are typical amino and alkyl multiple absorption bands at 3300–3500 and 2850–3050 cm^{-1}, respectively. Fig. 2(A) shows the ^{1}H-NMR spectrum of monomer **1**. The proton signals of amino groups can be found at 4.62 ppm, and the proton signals of *tert*-butyl and methyl groups appear at 1.20 and 1.97 ppm, respectively. The proton signals of H_c, H_d, and H_e on aminobenzene ring shift to high field due to electron donation effect of amino groups and methyl groups, and their chemical shifts appear at 6.48, 6.56, and 6.68 ppm, respectively. Fig. 2(B) is the ^{13}C-NMR spectrum of monomer **1**. The carbon absorption signals in the spectra are reasonably assigned, and all carbon signals on aromatic rings appear at 149.84, 144.93, 144.52, 133.34, 131.10, 127.48, 123.54, 121.04,

https://doi.org/10.1007/s10118-020-2377-y

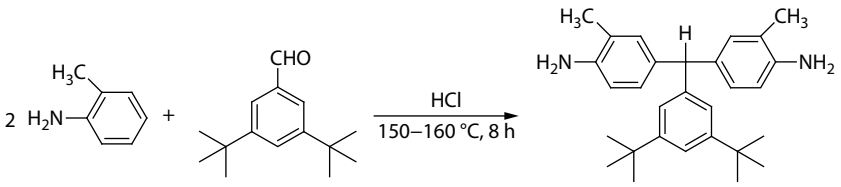

Scheme 1 Synthesis of aromatic diamine monomer **1**.

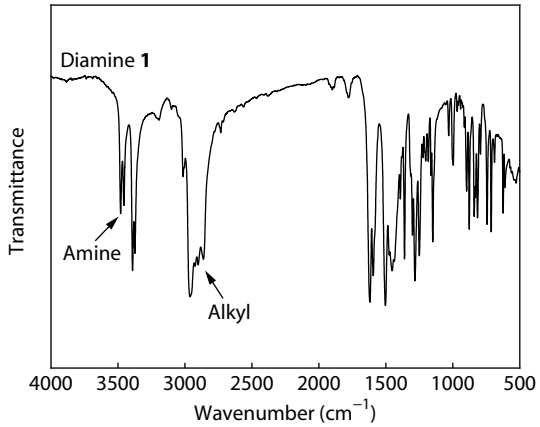

Fig. 1 FTIR spectrum of diamine **1**.

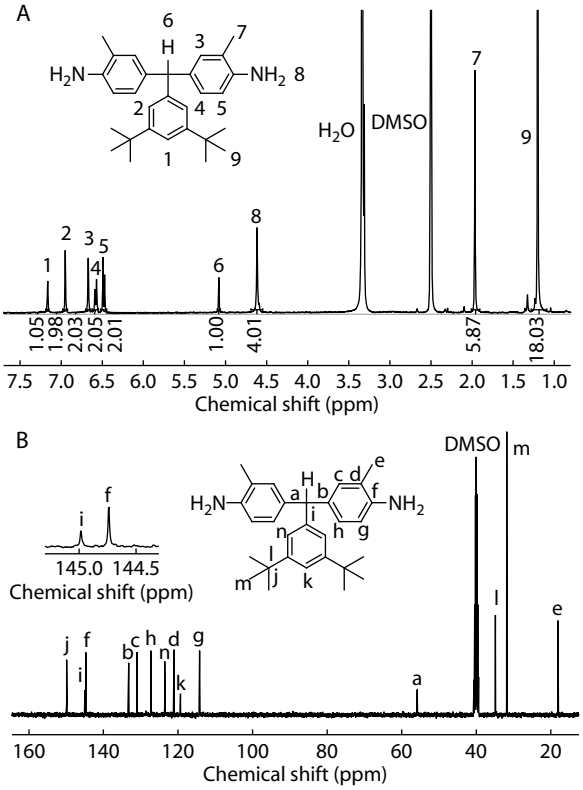

Fig. 2 ^{1}H- (A) and ^{13}C-NMR (B) spectra of monomer **1**.

119.38, and 114.33 ppm, respectively. The signals of alkyl carbon appear at 55.91, 34.93, 31.58, and 18.16 ppm, respectively. FTIR and NMR results confirmed that the diamine monomer with the designed structure has been obtained.

Synthesis of Polymers

PI 3a–**3c** were synthesized from aromatic diamine **1** and three aromatic dicarboxylic anhydrides (BPDA, ODPA, and 6FDA) by one-step solution condensation method. The synthetic route is shown in Scheme 2. *m*-Cresol and isoquinoline were used as solvents and catalysts, respectively. The polymerization was carried out at 195 °C in nitrogen atmosphere, and a small amount of water was continuously discharged from the system during the reaction until a uniform and viscous polymer solution was obtained eventually. Table 1 shows the intrinsic viscosity and relative molecular weights of the obtained polymers. The intrinsic viscosities of these polyimides in DMAc ranged from 0.53 dL·g^{-1} to 0.72 dL·g^{-1}. Their M_w and M_n values dissolved in THF were 7.3 × 10^4–1.25 × 10^5 and 3.6 × 10^5–4.8 × 10^5 g·mol^{-1}, respectively, and the polydispersity index (PDI) values were ranged from 2.0 to 2.6. The above results indicated that these polyimides were successfully prepared with moderate molecular weight and molecular weight distribution.

Fig. 3 shows the FTIR spectra of the prepared polymers. From the infrared spectra, it can be seen that the characteristic absorption bands of amino groups at 3200–3500 cm^{-1} disappear in all polymers, which indicates that the amino groups completely participated in the reaction. Typical characteristic bands of alkyl C—H appear at 2700–3100 cm^{-1}. The bands at 1779, 1724, and 1619 cm^{-1} are characteristic absorption bands of C=O on the imide ring, and the band at 1373 cm^{-1}

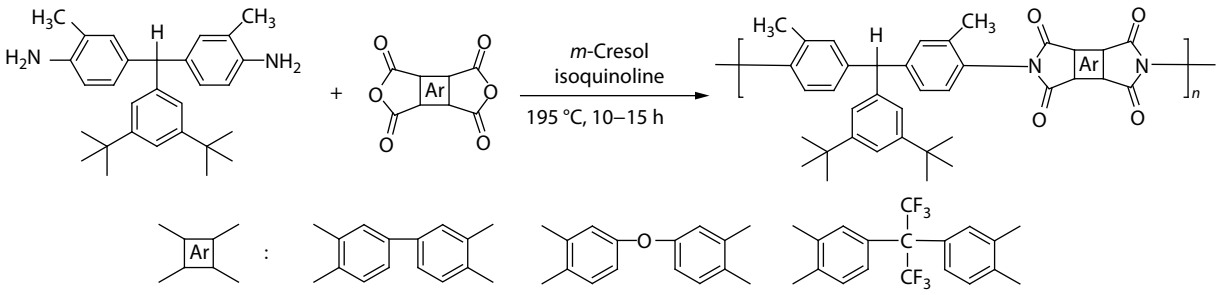

Scheme 2 Synthesis of polyimides (**PI 3a**–**3c**).

https://doi.org/10.1007/s10118-020-2377-y

Table 1 Inherent viscosities and molecular weights of polyimides.

Polymer	η_{inh} (dL·g^{-1})	GPC [a]		
		$M_n \times 10^{-4}$ (g·mol^{-1})	$M_w \times 10^{-4}$ (g·mol^{-1})	PDI
PI 3a	0.72	4.2	11.7	2.5
PI 3b	0.66	4.8	12.5	2.6
PI 3c	0.53	3.6	7.3	2.0

[a] Using polystyrene as a standard and THF as an eluent.

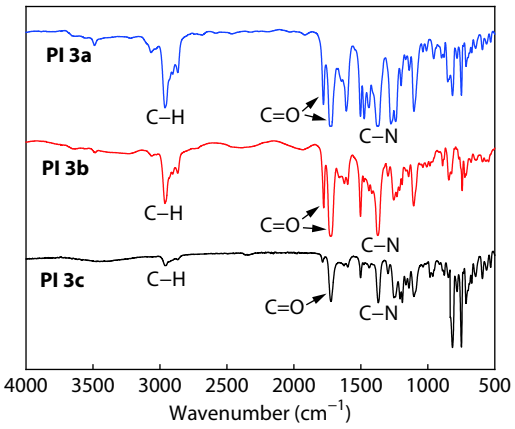

Fig. 3 FTIR spectra of **PI 3a**–**3c**.

is the stretching vibration characteristic of C—N on the imide ring. Fig. 4 shows the ^{1}H-NMR analysis of three polymers, and the corresponding proton signals are fully marked. It can be seen from Fig. 4 that the resonance signal of amino protons at 4.62 ppm in the NMR spectrum of diamine monomer has completely disappeared in the ^{1}H-NMR spectra of the polymers, which further confirmed the diamine monomer reacts with anhydrides completely to form imide groups. The proton signals of *tert*-butyl, methyl, and methylene can be observed at 1.35, 2.12, and 5.68 ppm, respectively. The proton signals of the dianhydride structure units appear at 7.72–8.34 ppm, and the proton signals of the diamine structure unit appear at 7.09–7.48 ppm. Due to the de-shielding effect caused by strong electron withdrawing of imide rings, the proton at position 4 in diamine structure units shifts to a low field and appears at chemical shift of 7.42 ppm.

Solubility

Aromatic polyimides were often insoluble in common organic solvents because of their rigidity and strong chain-to-chain interaction, which makes it difficult to prepare membranes directly. Table 2 shows the solubility testing results of these prepared polyimides in common organic solvents. It can be seen that the prepared polyimides show excellent solubility not only in some high boiling-point solvents such as DMF, NMP, DMAc, and *m*-cresol, but also in some low boiling-point solvents

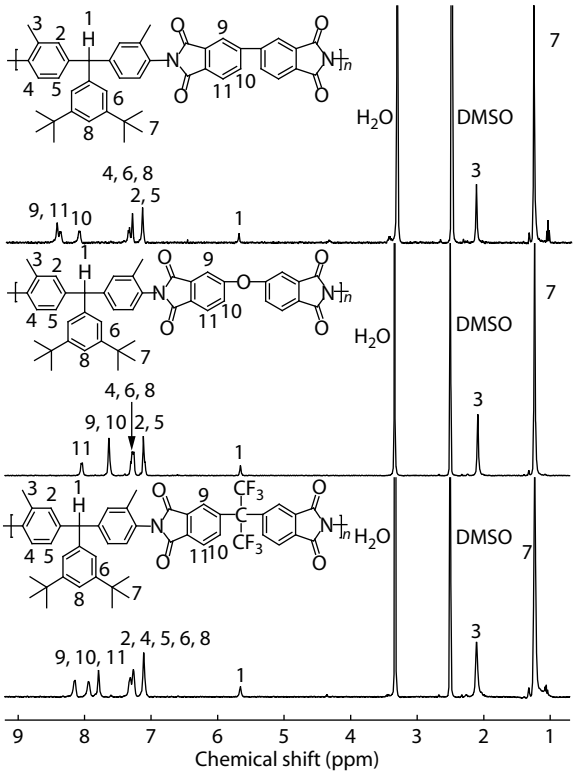

Fig. 4 ^{1}H-NMR spectra of **PI 3a**–**3c** in DMSO-d$_6$.

such as $CHCl_3$, CH_2Cl_2, and THF. Their solubility can even be greater than 10 wt%. From the microscopic point of view, the dissolution process of the polymer mainly includes the infiltration of solvent molecules and the swelling and dispersion of macromolecular chains. Therefore, the solubility of polymers is closely related to the close packing and the interaction between macromolecular chains. By introducing large substituted side groups such as di-*tert*-butylbenzene and dimethyl substituents into the molecular structure unit of **PI 3a**–**3c**, the close packing of macromolecular chains and the interaction between macromolecules are effectively reduced, so that the solubility of the prepared **PI 3a**–**3c** is better improved. Due to the further introduction of a larger free volume of trifluoromethyl groups in the dianhydride structure unit, **PI 3c** exhibited higher solubility in DMF and DMSO than other two polyimides did. Compared with some reported polyimides with large side group structures, this series of polyimides have better solubility in some solvents due to the larger free volume of di-*tert*-butylbenzene.[28–32] For example, Li *et al.* prepared a diamine monomer containing *tert*-butyl groups, of which the synthesized polyimides also exhibited good solubility in most solvents, but the polyimides based on BPDA needed heating when dissolved in some solvents such as DMAc, NMP, and THF.[28]

Table 2 Solubility behavior of PIs.

Polymer	DMF	NMP	DMAc	DMSO	$CHCl_3$	CH_2Cl_2	*m*-Cresol	THF	Ethanol
PI 3a	++	+++	+++	+/–	+++	+++	+++	+++	–
PI 3b	++	+++	+++	++	+++	+++	+++	+++	–
PI 3c	+++	+++	+++	++	+++	+++	+++	+++	–

+++, 100 mg of sample dissolved in 1 mL of solvent at room temperature (10 wt%); ++, dissolved when heated; +/–, partly dissolved when heated; –, insoluble.

https://doi.org/10.1007/s10118-020-2377-y

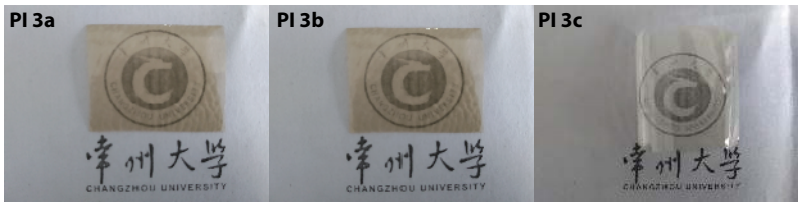

Fig. 5 Appearance images of three different polyimide membranes.

Table 3 Mechanical and optical properties of the PI membranes.

Polymer	Tensile strength (MPa)	Initial modulus (GPa)	Elongation at break (%)	λ_{cutoff} (nm)	$\lambda_{80\%}$ (nm)
PI 3a	76.9	1.8	4.9	339	543
PI 3b	87.3	1.7	6.1	348	521
PI 3c	77.7	1.7	5.9	310	423

Mechanical and Optical Properties

PI 3a–**3c** can be conveniently prepared into flexible and tough membranes with controllable thickness and light color through their polymer solution casting. Fig. 5 gives the appearance photos of these polyimide membrane samples. Their mechanical properties were tested and the results are shown in Table 3. The three polymers exhibit high tensile strength ranged from 76.9 MPa to 87.3 MPa. Their elastic modulus and elongation at break ranged from 1.7 GPa to 1.8 GPa and 4.9% to 6.1%, respectively. **PI 3b** has the highest elongation at break due to the introduction of flexible ether bond in dianhydride structure units. The existence of flexible bond enhances the ductility of polyimides.

The optical transparency of the prepared polyimides was tested and analyzed by ultraviolet-visible spectrometry (Fig. 6), and the results are given in Table 3. These polymer membranes have good optical transparency. Their UV cut-off wavelength is in the range of 310–348 nm, and the wavelength at 80% transmittance rate ($\lambda_{80\%}$) is in the range of 423–543 nm. Optical transparency is mainly related to the aromatic conjugation of polymer molecular chains and the intensity of charge-transfer complex (CTC) in the molecular chains.[33,34] With the introduction of di-*tert*-butylbenzene and dimethyl groups, the polymer molecular chains would exhibit a spatially distorted non-coplanar structure due to the steric hindrance effect of substituents (Fig. 7), which effectively reduces the aromatic conjugation and charge transfer of polymer molecular chains. So the optical transparency of these polyimides was improved obviously. **PI 3c** exhibited better optical transparency than other two polyimides did because the introduction of $-CF_3$ in the dianhydride structure units further increased steric hindrance effect and reduced intermolecular CTC effect, which also made the membrane the closest to colorless transparency. Compared to some reported polyimide membranes with other large substituted structures, the prepared polyimides have lower cut-off wavelength and higher optical transparency.[32,35,36] For example, Zhang *et al.* synthesized polyimides with trisphenol structure, of which the UV cut-off wavelength is about 360 nm, and the wavelength at 80% transmittance is about 610 nm, obviously higher than those of this series of polyimide membranes.[32] The excellent optical properties of **PI 3a**–**3c** could be attributed to the special modification effect of di-*tert*-butyl groups. In addition, compared with some modified fluorine-containing high transparent polyimide membranes reported in recent years,[37–40] the prepared polyimide membranes also have considerable cut-off wavelength and optical transparency, which further show that considerable modification effects can be obtained by introducing large substituted *tert*-butyl groups.

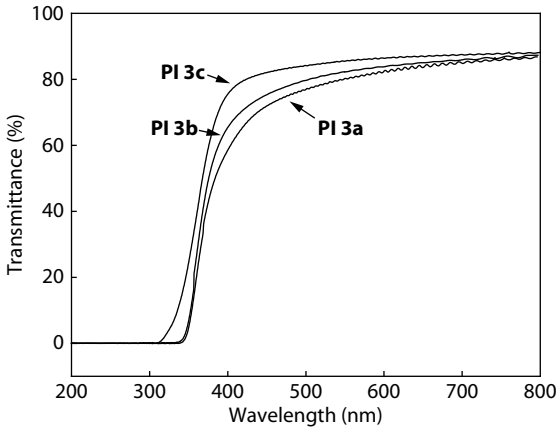

Fig. 6 UV-Vis spectra of the PI membranes.

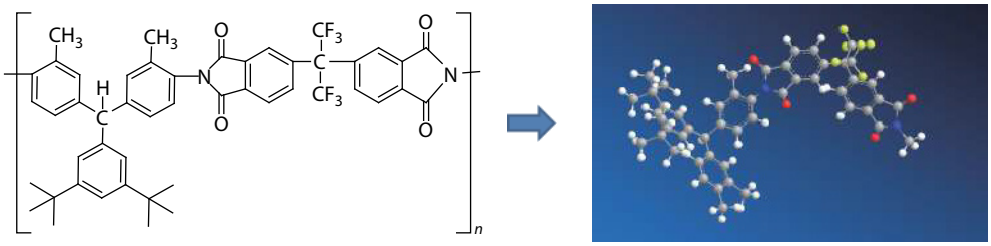

Fig. 7 Molecular structure and model diagram of **PI 3c.**

https://doi.org/10.1007/s10118-020-2377-y

Thermal Properties

The thermal properties of **PI 3a**–**3c** were analyzed by TGA and DSC. The testing results are shown in Table 4. The glass transition temperatures (T_g) of these polyimides are in the range of 264–302 °C, in which **PI 3b** shows the lowest T_g due to the flexible ether bond in the dianhydride structure unit, and **PI 3a** shows the highest T_g with a value of 302 °C due to the rigid biphenyl structure. Compared with some polyimides based on the same dianhydride monomers, it is found that these polyimides have higher glass transition temperatures (20–30 °C higher).[41–44] The higher glass transition temperatures of **PI 3a**–**3c** are mainly attributed to the rigidity of the diamine structure units. Meanwhile, the introduction of di-*tert*-butylbenzene and dimethyl group further hinders the internal rotation of polymer molecular chains due to steric hindrance effect, which could increase the rigidity of polymer chains and the glass transition temperature. The thermogravimetric temperatures of these polymers in N_2 and air atmosphere are all above 436 °C, and the residual sample masses at 800 °C in N_2 atmosphere are above 48%. The results of TGA test indicated that these polyimides have high heat resistance. Compared with other polyimides containing alkyl substituted structures, these polyimides have considerable degree of thermal decomposition temperatures.[41,45,46] As reported by Belov *et al.*, the polyimides containing multiple alkyl substituents have thermal decomposition temperature of about 420 °C at 10% weight loss.[41]

Table 4 Thermal properties of PIs.

Polymer	T_g (°C)	T_{d10} [a] (°C)		Char yield [b] (%)
		In N_2	In air	
PI 3a	302	525	436	52
PI 3b	264	522	446	50
PI 3c	282	526	440	59

[a] 10% Weight loss temperature in TGA; [b] Residual weight retention at 800 °C in nitrogen.

Crystallinity and Fractional Free Volume (FFV)

The density, free volumes and *d*-spacing of **PI 3a**–**3c** are shown in Table 5. Their density is in the range of 1.19–1.30 g·cm^{-3}, and the free volume fraction is in the range of 0.097–0.122. It can be seen that **PI 3c** has the lowest density and the largest free volume fraction compared with those of the other two polyimides, which is mainly attributed to the relatively large free volume of diphenyl hexafluoroisopropane in the dianhydride structure unit. Fig. 8 shows the wide-angle X-ray diffraction patterns of these polymers. It can be seen that the diffraction peaks of **PI 3a**–**3c** are wide dispersion peaks, showing amorphous properties. The amorphous property is mainly due to the introduction of di-*tert*-butylbenzene and dimethyl groups with large free volume, which together effectively destroy the regularity of the polymer chain and make the polymer present amorphous structure. It is also conducive to improving the solubility and membrane formation of the prepared polymers. It is well known that the position of the maximum value in the dispersion peak of X-ray diffraction pattern is considered to be the most probable distance between segments of polymer chains.[46] The *d*-spacing between peak A (*d*-A) and B (*d*-B) in Fig. 8 represents the distance between loosely packed and closely packed chains, respectively. The *d*-spacing of peak C (*d*-C) at about $2\theta = 27°$ can be attributed to the accumulation of π-π of imides and phenyl aromatic heterocycles in the polymer skeleton. The *d*-spacing values of these polymers are 5.61, 5.40, and 5.88 Å, respectively, which indicates the polymer chains are loosely packed. The increasing order of *d*-spacing (**PI 3c** > **PI 3a** > **PI 3b)** is closely related to the dianhydride structural units in polymer skeleton. In this study, the *d*-spacing of polyimides is at a considerable level compared with those of other polyimides with *tert*-butyl groups. For example, Sulub *et al.* synthesized polyimides based on dianhydride monomer with di-*tert*-butyl structure, and their *d*-spacing values were between 5.21–6.02 Å.[22] Therefore, it is not difficult to conclude that the introduction of several pendant groups in diamine monomers or dianhydride monomers can inhibit the close packing of polymer molecular chains, which increases the molecular chain spacing.

Gas Transport Properties

Table 6 shows the permeability coefficients of the obtained polyimide membranes for four different gases (CO_2, O_2, N_2, and CH_4) and their selective separation coefficients for different gas pairs. The gas separation properties data for the comparative Kapton, Matrimid, and some polyimides reported are also listed in Table 6. The results show that the order of permeability of these prepared polyimides for different gases is $P(CO_2) > P(O_2) > P(N_2) > P(CH_4)$, which is the opposite of their order of dynamical diameter. The permeability coefficients of these polyimides for CO_2 and O_2 were in the range of 101.9–124.6 barrer and 33.3–42.8 barrer, respectively. The selective separation coefficients for CO_2/CH_4 and O_2/N_2 were in the range of 13.01–14.99 and 3.29–4.22, respectively. Among these polyimide membranes, **PI 3c** exhibits the highest permeability coefficient, which is consistent with its large free volume and low density.

Permeability coefficient, as an important criterion of polymer separation membranes, plays a decisive role in the application of polymer membranes.[48–50] Modern high-efficiency gas separation equipment usually requires polymer membranes with high permeability coefficient in order to improve the efficiency of gas separation. Compared with typical Kapton and Matrimid polyimides with spiral structures, it can be found that **PI 3a**–**3c** membranes have much higher permeability, which is mainly attributed to the introduction of large free volume side groups in diamine structure units. In addition, compared to some modified fluorinated polyimide membranes based on 4,4′-(hexafluoroisopropylidene)diphthalic anhydride and polyimide membranes containing di-

Table 5 Physical properties of the polyimides.

Polymer	ρ [a] (g·cm^{-3})	V (cm^3·mol^{-1})	Vw (cm^3·mol^{-1})	FFV	2θ (°)	*d*-spacing (Å)
PI 3a	1.28	525.31	364.59	0.097	15.77	5.61
PI 3b	1.30	529.23	363.13	0.108	16.41	5.40
PI 3c	1.19	691.60	466.56	0.122	15.05	5.88

[a] The density of the membranes in the hydroxide form was measured by buoyancy method.

https://doi.org/10.1007/s10118-020-2377-y

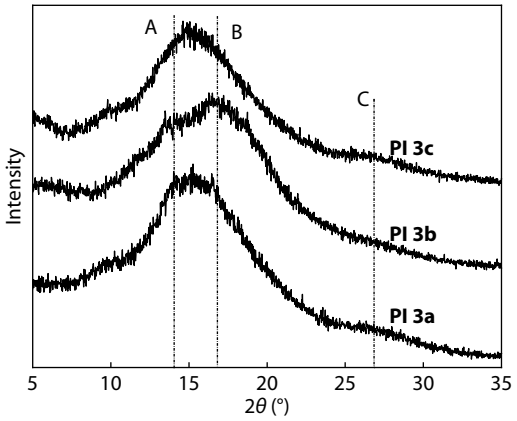

Fig. 8 Wide-angle X-ray diffraction patterns of polyimide membranes.

tert butyl side groups, the permeability of these prepared polyimide has also been significantly improved. For example, the permeability coefficients of 6FDA-FSBC, 6FDA-SBC, and 6FDA-MSBC for CO_2 are in the range of 21.2–66.0 barrer, while the permeability coefficient of **PI 3c** for CO_2 is 124.6 barrer. The selective separation coefficients of PMDA-TBAPB, BPDA-TBAPB, and 6FDA-TBAPB for O_2/N_2 are in the range of 3.59–5.41, which stands as at the same level as **PI 3a**–**3c**. The above results further suggest that the introduction of di-*tert*-butylbenzene and dimethyl side groups in diamine structure unit has good modification effect.

The trade-off between gas permeability and selectivity theoretically implies high permeability but low selectivity, which is also reflected in **PI 3a**–**3c** data. Early reports indicate that gas permeability depends on the free volume of the polymer and can be calculated according to an empirical formula: $P = A\exp(-B/FFV)$, where A is a coefficient and B is the molar volume of penetrant.[46] It is concluded that the logarithm of permeability increases linearly with increasing reciprocal of free volume for different polymer systems. Fig. 9 further studies the relationship between permeability and selectivity of these membranes for O_2/N_2 and CO_2/CH_4 gas pairs, using Robeson upper bound in 2008 as a reference. It can be clearly seen that all three polyimides have good selectivity for O_2/N_2 gas. The permeability coefficient of **PI 3c** is not only better than that of some other polyimides, but also very close to Robeson upper bound, which makes this polymer membrane have good potential application prospects in the field of O_2 collection.

CONCLUSIONS

In this work, a novel aromatic diamine monomer containing pendant di-*tert*-butylbenzene and dimethyl groups was successfully synthesized by a convenient coupling reaction. Three polyimides **PI 3a**–**3c** were prepared from the obtained diamine monomer and a series of commercialized dianhyd-

Table 6 Gas permeability coefficients (P) in barrer and permselectivities (α) of the polyimides and their comparison with some polyimides reported earlier.

Polymer	$P(CO_2)$	$P(CH_4)$	$P(O_2)$	$P(N_2)$	$\alpha(CO_2/CH_4)$	$\alpha(O_2/N_2)$	$\alpha(CO_2/N_2)$	$\alpha(CO_2/O_2)$
PI 3a	109.3	8.4	36.6	9.9	13.01	3.70	11.04	2.99
PI 3b	101.9	6.8	33.3	7.9	14.99	4.22	12.90	3.06
PI 3c	124.6	8.5	42.8	13	14.66	3.29	9.59	3.37
Kapton[46]	3.50	0.06	0.64	0.11	58.5	5.82	31.90	5.48
Matrimid[46]	8.70	0.24	1.90	0.27	36.25	7.04	32.22	4.58
6FDA-FSBC[46]	66.0	2.5	17.0	3.7	25.88	4.61	17.89	3.88
6FDA-SBC[46]	32.1	1.3	8.2	1.9	25.08	4.38	17.17	3.92
6FDA-MSBC[46]	21.2	0.77	5.6	1.4	27.53	3.91	14.93	3.82
PMDA-TBAPB[47]	141.8	7.84	22.9	5.79	18.1	3.59	24.49	6.19
BPDA-TBAPB[47]	19.6	0.88	5.09	0.94	22.2	5.41	20.85	3.85
6FDA-TBAPB[47]	42.4	4.65	10.1	1.96	25.7	5.17	21.63	4.19

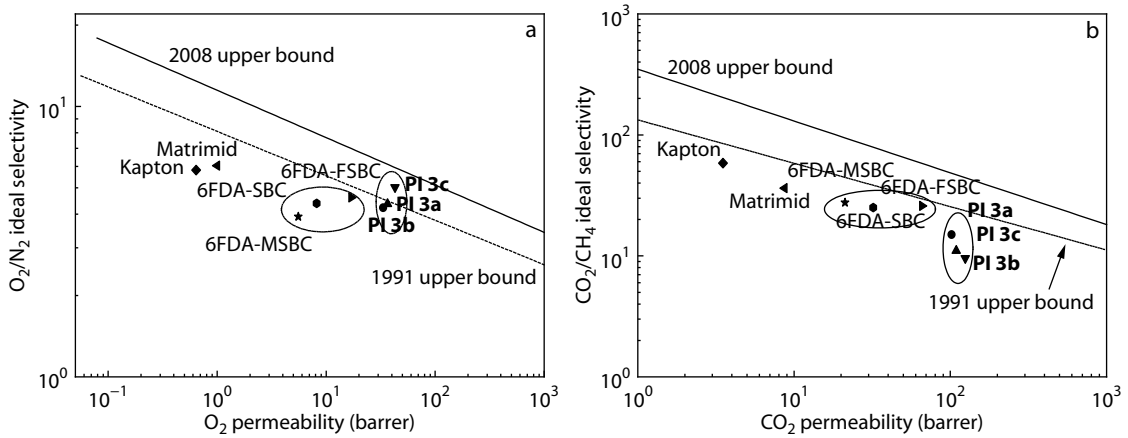

Fig. 9 Separation performance for O_2/N_2 (a) and CO_2/CH_4 (b) gas pairs showing data for **PI 3a**–**3c** and some references.

https://doi.org/10.1007/s10118-020-2377-y

ride monomers by one-step high-temperature polymerization. This kind of polyimides exhibited good solubility, which can be dissolved in most organic solvents at room temperature. All the PIs possessed good heat resistance with high T_g values. The prepared membranes have better optical transparency and gas permeability compared with those of some modified polyimides reported in recent years. The selective permeability of **PI 3c** to O_2/N_2 is close to the upper bound of Robeson in 2008. The better gas permeability is mainly attributed to the introduction of di-*tert*-butylbenzene and dimethyl groups, which reduces the close packing of macromolecular chains and gives the polymer higher free volume. This study could provide a new strategy and methodology for the design and preparation of high performance polyimide membranes with *tert*-butyl structure.

ACKNOWLEDGMENTS

This work was financially supported by the Key Research Project of Jiangsu Province (No. BE2017645), Scientific Research and Innovation Project for Graduate Students in Jiangsu Province (No. KYCX19-1757), and a Project Funded by the Priority Academic Program Development of Jiangsu Higher Education Institutions of China.

REFERENCES

1 Mosanenzadeh, S. G.; Saadatnia, Z.; Shi, F.; Park, C. B.; Naguib, H. E. Structure to properties relations of BPDA and PMDA backbone hybrid diamine polyimide aerogels. *Polymer* **2019**, *176*, 213–226.
2 Jia, M.; Zhou, M.; Li, Y. J.; Lu, G. L.; Huang, X. Y. Construction of semi-fluorinated polyimides with perfluorocyclobutyl aryl ether-based side chains. *Polym. Chem.* **2018**, *9*, 920–930.
3 Qu, L.; Tang, L.; Bei, R.; Zhao, J.; Chi, Z.; Liu, S.; Chen, X.; Aldred, M. P.; Zhang, Y.; Xu, J. Flexible multifunctional aromatic polyimide film: highly efficient photoluminescence, resistive switching characteristic, and electroluminescence. *ACS Appl. Mater. Interfaces* **2018**, *10*, 11430–11435.
4 Wang, C. Y.; Chen, W. T.; Xu, C.; Zhao, X. Y.; Li, J. Fluorinated polyimide/POSS hybrid polymers with high solubility and low dielectric constant. *Chinese J. Polym. Sci.* **2016**, *34*, 1363–1372.
5 Wang C. Y.; Zhao, X. Y.; Li, G.; Jiang, J. M. High optical transparency and low dielectric constant of novel soluble polyimides containing fluorine and trifluoromethyl groups. *Colloid Polym. Sci.* **2011**, *289*, 1617–1624.
6 Liu, Y. W.; Tang, L. S.; Qu, L. J. Synthesis and properties of high performance functional polyimides containing rigid nonplanar conjugated fluorene moieties. *Chinese J. Polym. Sci.* **2019**, *37*, 416–427.
7 Yong, W. F.; Li, F. Y.; Chung, T. S.; Tong, Y. W. Highly permeable chemically modified PIM-1/Matrimid membranes for green hydrogen purification. *J. Mater. Chem. A* **2013**, 13914–13925.
8 Li, N. B.; Wang, M.; Guo, L. X.; Lin, B. P.; Yang, H. Ionic liquid embedded polyimides with ultra-foldability, ultra-flexibility, ultra-processability and superior optical transparency. *Polymer* **2018**, *153*, 538–547.
9 Wu, Z. L.; Han, B. C.; Zhang, C. H.; Zhu, D. Y.; Gao, L. X.; Ding, M. X.; Yang, Z. H. Novel soluble and optically active polyimides containing axially asymmetric 9,9′-spirobifluorene units: synthesis, thermal, optical and chiral properties. *Polymer* **2012**, *53*, 5706–5716.
10 Genduso, G.; Wang, Y. G.; Ghanem, B. S.; Pinnau, I. Permeation, sorption, and diffusion of CO_2-CH_4 mixtures in polymers of intrinsic microporosity: the effect of intrachain rigidity on plasticization resistance. *J. Membr. Sci.* **2019**, *584*, 100–109.
11 Wang, C. Y.; Zhao, X. Y.; Li, G. Synthesis and properties of new fluorinated polyimides derived from an unsymmetrical and noncoplanar diamine. *Chin. J. Chem.* **2012**, *30*, 2466–2472.
12 Wang, C. Y.; Zhao, X. Y.; Li, G. New soluble polyimides with high optical transparency and light color containing pendant trifluoromethyl and methyl groups. *Chin. J. Chem.* **2012**, *30*, 1555–1560.
13 Ghanem, B. S.; McKeown, N. B.; Budd, P. M.; Selbie, J. D.; Fritsch, D. High-performance membranes from polyimides with intrinsic microporosity. *Adv. Mater.* **2008**, *20*, 2766–2771.
14 Zhang, R.; Li, T. Y.; Zhou, H. B.; Huang, H. H.; Chen, Y. M. Biobased transparent polyimides with excellent solubility and mechanical properties using myo-inositol derived diamines. *React. Funct. Polym.* **2018**, *128*, 91–96.
15 Wang, C. Y.; Cao, S. J.; Chen, W. T.; Zhao, X. Y.; Li, J.; Ren, Q. A series of soluble polyimides containing sulfone and trifluoromethyl groups. *J. Changzhou Univ. (Natural Science Edition)* **2018**, *30*, 7–12.
16 Wang, C.; Li, G.; Jiang, J. Novel soluble polyimide containing 4-*tert*-butyltoluene moiety: synthesis and characterization. *Chin. J. Chem.* **2009**, *27*, 2255–2260.
17 Gan, C. J.; Xu, X. C.; Jiang, X. W. Fabrication of 6FDA-HFBAPP polyimide asymmetric hollow fiber membranes and their CO_2/CH_4 separation properties. *Chinese J. Polym. Sci.* **2019**, *37*, 815–826.
18 Sanaeepur, H.; Ebadi,; Amooghin, A.; Bandehali, S.; Moghadassi, A.; Matsuura, T.; Bruggen, B. V. Polyimides in membrane gas separation: monomer's molecular design and structural engineering. *Prog. Polym. Sci.* **2019**, *91*, 80–125.
19 Ghanem, B. S.; Swaidan, R.; Litwiller, E.; Pinnau, I. Ultra-microporous triptycene-based polyimide membranes for high-performance gas separation. *Adv. Mater.* **2014**, *26*, 3688–3692.
20 Baker, R. W.; Lokhandwala, K. Natural gas processing with membranes: an overview. *Ind. Eng. Chem. Res.* **2008**, *47*, 2109–2121.
21 Sanders, D. F.; Smith, Z. P.; Guo, R.; Robeson, L. M.; Mcgrath, J. E.; Paul, D. R.; Freeman, B. D. Energy-efficient polymeric gas separation membranes for a sustainable future: a review. *Polymer* **2013**, *54*, 4729–4761.
22 Wu, Z.; Yan, G.; Lu, J.; Zhang, G.; Yang, J. Thermal plastic and optical transparent polyimide derived from isophorone diamine and sulfhydryl compounds. *Ind. Eng. Chem. Res.* **2019**, *58*, 6992–7000.
23 Sulub-Sulub, R.; Loría-Bastarrachea, M. I.; Vázquez-Torres, H.; Santiago-García, J. L.; Aguilar-Vega, M. Highly permeable polyimide membranes with a structural pyrene containing tert-butyl groups: synthesis, characterization and gas transport. *J. Membr. Sci.* **2018**, *563*, 134–141.
24 Qiu, Z. M.; Chen, G.; Zhang, Q. Y.; Zhang, S. B. Synthesis and gas transport property of polyimide from 2,2′-disubstituted biphenyltetracarboxylic dianhydrides (BPDA). *Eur. Polym. J.* **2007**, *43*, 194–204.
25 Nikiforov, R.; Belov, N.; Zharov, A.; Konovalova, I.; Shklyaruk, B.; Yampolskii, Y. Gas permeation and diffusion in copolymers of tetrafluoroethylene and hexafluoropropylene: effect of annealing. *J. Membr. Sci.* **2017**, *540*, 129–135.
26 Bondi, A. van der Waals volumes and radii. *J. Phys. Chem.* **1964**, *68*, 441–451.
27 Park, J. Y.; Paul, D. R. Correlation and prediction of gas permeability in glassy polymer membrane materials *via* a modified free volume based group contribution method. *J. Membr. Sci.* **1997**, *125*, 23–29.

https://doi.org/10.1007/s10118-020-2377-y

28 Yi, L.; Li, C.; Huang, W. Soluble polyimides from 4,4′-diaminodiphenyl ether with one or two *tert*-butyl pedant groups. *Polymer* **2015**, *80*, 67–75.
29 Zhao, Q.; Wang, X. Y.; Hu, Y. H. The application of highly soluble amine-terminated aromatic polyimides with pendent *tert*-butyl groups as a tougher for epoxy resin. *Chinese J. Polym. Sci.* **2015**, *33*, 1359–1372.
30 Ishii, J.; Takata, A.; Oami, Y.; Yokota, R.; Vladimirov, L.; Hasegawa, M. Spontaneous molecular orientation of polyimides induced by thermal imidization (6). Mechanism of negative in-plane CTE generation in non-stretched polyimide membranes. *Eur. Polym. J.* **2010**, *46*, 681–693.
31 Qiu, Z. M.; Zhang, S. B. Synthesis and properties of organosoluble polyimides based on 2,2′-diphenoxy-4,4′,5,5′-biphenyltetracarboxylic dianhydride. *Polymer* **2005**, *46*, 1693–1700.
32 Zhang, Q. Y.; Li, S. H.; Li, W. M.; Zhang, S. B. Synthesis and properties of novel organosoluble polyimides derived from 1,4-bis[4-(3,4-dicarboxylphenoxy)]triptycene dianhydride and various aromatic diamines. *Polymer* **2007**, *48*, 6246–6253.
33 Yang, C. P.; Hsiao, S. H.; Chen, K. H. Organosoluble and optically transparent fluorine-containing polyimides based on 4,4′-bis(4-amino-2-trifluoromethylphenoxy)-3,3′,5,5′-tetramethylbiphenyl. *Polymer* **2002**, *43*, 5095–5104.
34 Wang, C. Y.; Chen, W. T.; Chen, Y. Y.; Zhao, X. Y.; Li, J.; Ren, Q. Synthesis and properties of new fluorene-based polyimides containing trifluoromethyl and isopropyl substituents. *Mater. Chem. Phys.* **2014**, *144*, 553–559.
35 Liu, J. T.; Chen, G. F.; Guo, J. C.; Mushtaq, N.; Fang, X. Z. Synthesis of high performance phenolphthalein-based cardo poly(ether ketone imide)s *via* aromatic nucleophilic substitution polymerization. *Polymer* **2015**, *70*, 30–37.
36 Mo, X.; Wang, C. Y.; Li, G.; Jiang, J. M. High optical transparency and low dielectric constant polyimides containing trifluoromethyl and cyclohexane groups. *J. Macromol. Sci. Phys.* **2011**, *51*, 1370–1383.
37 Yang, C. P.; Hsiao, S. H.; Wu, K. L. Organosoluble and light-colored fluorinated polyimides derived from 2,3-bis(4-amino-2-trifluoromethylphenoxy)naphthalene and aromatic dianhydrides. *Polymer* **2003**, *44*, 7067–7078.
38 Yang, C. P.; Hsiao, S. H.; Hsu, M. F. Organosoluble and light-colored fluorinated polyimides from 4,4′-bis(4-amino-2-trifluoromethylphenoxy) biphenyl and aromatic dianhydrides. *Polym. Chem.* **2002**, *40*, 524–534.
39 Liu, H.; Zhai, L.; Bai, L.; He, M. H.; Wang, C. G.; Mo, S.; Fan, L. Synthesis and characterization of optically transparent semi-aromatic polyimide films with low fluorine content. *Polymer* **2019**, *163*, 106–114.
40 Wang, C.; Cao, S.; Chen, W.; Xu, C.; Zhao, X.; Li, J.; Ren, Q. Synthesis and properties of fluorinated polyimides with multi-bulky pendant groups. *RSC Adv.* **2017**, *7*, 26420–26427.
41 Belov, N.; Chatterjee, R.; Nikiforov, R.; Ryzhikh, V.; Bisoi, S.; Kumar, A. G.; Banerjee, S.; Yampolskii, Y. New poly(ether imide)s with pendant di-*tert*-butyl groups: synthesis, characterization and gas transport properties. *Sep. Purif. Technol.* **2019**, *217*, 183–194.
42 Dhara, M. G.; Banerjee, S. Fluorinated high-performance polymers: poly(arylene ether)s and aromatic polyimides containing trifluoromethyl groups. *Prog. Polym. Sci.* **2010**, *35*, 1022–1077.
43 Barikani, M.; Mehdipour-Ataei, S. Synthesis, characterization, and thermal properties of novel arylene sulfone ether polyimides and polyamides. *J. Polym. Sci. Part A: Polym. Chem.* **2000**, *38*, 1487–1492.
44 Wang, C.; Chen, W.; Chen, Y.; Zhao, X.; Li, J.; Ren, Q. New fluorinated poly(ether sulfone imide)s with high thermal stability and low dielectric constant. *Mater. Chem. Phys.* **2014**, *143*, 773–778.
45 Tian, Z. K.; Cao, B.; Li, P. Effects of sub-T_g cross-linking of triptycene-based polyimides on gas permeation, plasticization resistance and physical aging properties. *J. Membr. Sci.* **2018**, *560*, 87–96.
46 Zhang, C.; Li, P.; Cao, B. Effects of the side groups of the spirobichroman-based diamines on the chain packing and gas separation properties of the polyimides. *J. Membr. Sci.* **2017**, *530*, 176–184.
47 Calle, M.; Lozano, A. E.; Abajo, J. D.; Campa, J. G. D.; Álvarez,; C,. Design of gas separation membranes derived of rigid aromatic polyimides. 1. Polymers from diamines containing di-*tert*-butyl side groups. *J. Membr. Sci* **2010**, *365*, 145–153.
48 Zhang, C. L.; Li, P.; Cao, B. Decarboxylation crosslinking of polyimides with high CO_2/CH_4 separation performance and plasticization resistance. *J. Membr. Sci.* **2017**, *528*, 206–216.
49 Jiang, X. W.; Xiao, X.; Xu, X. C. Effects of non-TR-able codiamines and rearrangement conditions on the chain packing and gas separation performance of thermally rearranged poly(benzoxazole-*co*-imide) membranes. *J. Membr. Sci.* **2018**, *564*, 605–616.
50 Duthie, X.; Kentish, S.; Powell, C.; Nagai, K.; Qiao, G.; Stevens, G. Operating temperature effects on the plasticization of polyimide gas separation membranes. *J. Membr. Sci.* **2007**, *294*, 40–49.

https://doi.org/10.1007/s10118-020-2377-y